This is a preprint, the final version is subject to change, of the American Mineralogist (MSA)
Cite as Authors (Year) Title. American Mineralogist, in press.
(DOI will not work until issue is live.) DOI: http://dx.doi.org/10.2138/am.2014.4772

Toward an accurate *ab initio* estimation of compressibility and thermal expansion of diamond in the [0, 3000K] temperature, and [0, 30GPa] pressures ranges, at the hybrid HF/DFT theoretical level

Mauro PRENCIPE[1], Marco BRUNO[1], Fabrizio NESTOLA[2], Marco DE LA PIERRE[3,4], Paolo NIMIS[2]

[1]Dipartimento di Scienze della Terra, University of Torino, Via Valperga Caluso 35, 10125 Torino, Italy
[2]Dipartimento di Geoscienze, University of Padova, Via Giotto 1, 35121 Padova, Italy
[3]Dipartimento di Chimica IFM, University of Torino, Via Giuria 1, 10125 Torino, Italy
[4]NIS - Nanostructured Interfaces and Surfaces Centre of Excellence, Via Giuria 7, 10125 Torino, Italy

ABSTRACT

The isothermal bulk modulus, together with its temperature dependence, and the thermal expansion of diamond at various pressures, were calculated from first principles in the [0, 30GPa] and [0, 3000K] pressure and temperature ranges, within the limits of the Quasi-Harmonic Approximation (QHA). The hybrid HF/DFT functional employed (WC1LYP) proved to be particularly effective in providing a very close agreement between the calculated and the available experimental data. In particular, the bulk modulus at 300K was estimated to be 444.6 GPa (K' = 3.60); at the same temperature, the (volume) thermal expansion coefficient was $3.19 \cdot 10^{-6}$ K^{-1}. To the authors' knowledge, among the theoretical papers devoted to the subject, the present one provides the most accurate thermo-elastic data in high pressure and temperature ranges. Such data can confidently be used in the determination of the pressure of formation using the "elastic method" for minerals found as inclusions in diamonds, thus shading light upon the genesis of diamonds in the Earth's upper mantle.

keywords: diamond, thermo-elastic properties, thermal expansion, ab initio calculations.

Always consult and cite the final, published document. See http://www.minsocam.org or GeoscienceWorld

INTRODUCTION

This work is part of a wider project devoted to the study of diamonds formation in the upper mantle and its growth relationships with those minerals that are commonly found as inclusions in diamonds. In particular, subcratonic diamonds can contain inclusions of other minerals like olivine, garnet, spinel, pyroxenes, sulfides (Nestola et al. 2011; Shirey et al. 2013). Diamonds and their inclusions are among the deepest materials originating from the Earth's interior and reaching the planet surface. Their study plays a key role in understanding and interpreting the geodynamics, geophysics, petrology, geochemistry and mineralogy of the Earth's mantle (Stachel and Harris 2008, and references therein). By the study of such inclusions, *in situ*, by means of diffrattometric or spectroscopic techniques, it is possible to determine the pressure (and the corresponding depth in the Earth’s mantle) at which the inclusions were formed (Nestola et al. 2011; Izraeli et al. 1999) using the so called “elastic method” (see Shirey et al. 2013 for a review). However, to this end, very accurate data concerning the pressure-volume equation of state, the thermal expansion and the bulk modulus temperature dependence of both diamond and its inclusions are absolutely crucial in order to obtain low error in the pressure of formation.

As concerns diamond, previous experimental and theoretical determinations of the elastic parameters and thermal expansion existed. In particular, from the experimental side, the elastic constants measurements from Brillouin scattering, at room or higher temperatures, allowed the estimation of the bulk modulus and its temperature dependence (Grimsditch and Ramdas 1975; McSkimin and Andreatch 1972; Vogelgesang et al. 1996; Zouboulis et al. 1998). Experimental thermal expansion data (from low to high temperature up to 3000K) at room pressure, are available from Stoupin and Shvyd’ko (2011), and from Reeber and Wang (1996). Due to technical difficulties in the experimental

Always consult and cite the final, published document. See http://www.minsocam.org or GeoscienceWorld

determinations of accurate bulk moduli and thermal expansion at simultaneous high pressure and temperature, a number of theoretical works were devoted to the subject, both at the ab initio level (Hebbache 1999; Kunc et al. 2003; Ivanova and Mavrin 2013; Maezono et al. 2007; Mounet and Marzari 2005; Valdez et al. 2012; Xie et al. 1999; Zhi-Jian et al. 2009) or the empirical one (force fields and other techniques based on some specific models; Aguado and Baonza 2006; Gao et al. 2006). Strongly depending upon the specific method employed, the calculated bulk moduli could be overestimated or underestimated by more than 10 GPa with respect to the experimental datum at 300K, so that a more reliable ab initio methodology is required to get values which could parallel the experimental techniques in accuracy and under very extreme conditions of P and T. To this end, the equation of state and the thermal expansion of diamond in the [0, 3000K] and [0, 30GPa] temperature and pressure ranges, respectively, have been determined by using the most recent ab initio techniques so far developed. In particular, an hybrid Hartree-Fock/Density Functional Theory (HF/DFT) functional has been employed. Hybrid functionals assure a very high accuracy in reproducing thermo-elastic parameters and vibrational properties of crystals, as it has already been proven in several papers (see for instance: De La Pierre et al. 2011a, Prencipe et al. 2011; Ungureanu et al. 2012; Zucchini et al. 2012; Scanavino et al. 2012; Prencipe et al. 2012a; Prencipe et al. 2012b, Scanavino and Prencipe 2013, and references therein).

COMPUTATIONAL DETAILS

Geometry optimization (cell parameter at the equilibrium), energy calculations at the static limit (no zero point and thermal energies) and vibrational frequencies calculations, for a set of different unit

Always consult and cite the final, published document. See http://www.minsocam.org or GeoscienceWorld

cell volumes, were performed by means of the CRYSTAL09 program (Dovesi et al. 2005; Dovesi et al. 2009). The chosen functional (WC1LYP) is a hybrid HF/DFT one, based on the WC (GGA) exchange functional proposed by Wu and Cohen (Wu and Cohen 2006), mixed with 16% of the exact non-local Hartree-Fock exchange, and employing the LYP correlation functional (Lee et al. 1988). Such percentage of exact Hartree-Fock exchange is essential for the correct reproduction of the elastic and vibrational properties of crystals, as demonstrated in previous works that had employed this functional (De La Pierre et al. 2011a; Demichelis et al. 2010; Prencipe et al. 2011; Prencipe 2012a; Prencipe et al. 2012b; Scanavino et al. 2012; Scanavino and Prencipe 2013; Ungureanu et al. 2010; Ungureanu et al. 2012; Zicovich-Wilson et al. 2004). With the purpose of testing and comparing our results with those reported from other Authors, static calculations were repeated by employing the B3PW (Becke 1993) and PBE functionals (Perdew et al. 1996). As the localized basis sets are concerned, a 6-111G* basis (B1 in the following), derived from the 6-21G* one by Dovesi et al. (1990) was mainly employed for the calculation of the zero point and thermal pressure contributions (see below), where the computational cost of the proper evaluation of dispersion effects in the phonon spectrum prevented us from the use of a very rich basis set. A very high quality basis set (B2 in the following), precisely a triple-zeta (TPZ) basis by Peintinger et al. (2013) having the (6211/411/1) structure, specifically designed for solid state calculations, was employed for the static equation of state (see below). Such basis is the one indicated as pob-TZVP basis in Table 2 of Peintinger et al. (2013); the notation to specify the basis indicates the number of contracted functions (s/p/d). To get more variational freedom and a better description of directional bonding situations like those in diamond, a B1' basis (6111/111/1) was also employed where, as in the case of the B2 basis and at variance with the B1 one, the n*s* and n*p* electrons ($n>2$) were associated with different Gaussian

Always consult and cite the final, published document. See http://www.minsocam.org or GeoscienceWorld

functions describing the radial part of the localized orbitals. More details about the procedure which has been followed to calculate energies and vibrational frequencies, and the computational parameters employed are provided in the Appendix. Static energies and vibrational frequencies at the different cell volumes are provided as supplementary material.

At each cell volume, the static, zero point and thermal pressure were computed following the algorithms fully described in Prencipe et al. (2011). The procedures to estimate the bulk modulus together with its pressure and temperature dependence, and the thermal expansion are also reported in Prencipe et al. (2011).

On the validity of the Quasi-harmonic Approximation

Since the Quasi-Harmonic Approximation (QHA) was extensively used to derive thermal pressures even at high temperatures, tests have been done to verify its validity even at those thermal conditions; indeed, as a rule of thumb, it is often claimed that such approximation can be safely applied at temperatures not higher than 2/3 of the melting temperature. Failures of the QHA at a given temperature, must clearly be seen in possible significant deviations of the Born-Oppenheimer (BO) surface from the harmonic shape, around the equilibrium positions of the nuclei, at the cell volume corresponding to the given temperature (and pressure). Such deviations, if any, are likely to be present in the cases of the low frequency modes, as the displacements of the nuclei along the corresponding normal mode coordinates are expected to be large and far away their equilibrium positions, thus exploring extended regions of the BO surface which could no longer be fitted by a harmonic expansion. A scan of the BO surface along the normal mode having the lowest frequency (283 cm^{-1}) computed in a diamond supercell, at a cell volume corresponding to a temperature of 3000K and a pressure of 0GPa, is reported in Figure 1: the continuous line represents the *exact* total

Always consult and cite the final, published document. See http://www.minsocam.org or GeoscienceWorld

energy as calculated, by the CRYSTAL09 program, by moving the nuclei point wise along the normal mode direction; the filled circles represent the energy values recalculated from a harmonic fit of the exact energy curve. No deviation at all of the BO, along the mode direction, from the harmonic shape is indeed observed, thus the validity of the QHA is clearly demonstrated even at 3000K and zero pressure. This is no wonder however, since the small thermal expansion of diamond even at high temperature, compared to those of the majority of other materials, is small (α=1.7·$10^{-5}$$K^{-1}$, at 3000K, see below): as the thermal expansion is one of the most apparent evidence of the deviation of the atomic interactions from the harmonic law (as it is well known, a perfectly harmonic crystal would have no thermal expansion at all), it is clear that in diamond such deviations are small even at high temperature, so that a QHA approach must be reasonably accurate.

RESULTS AND DISCUSSION

Equation of State

The discussion concerning the estimation of the equation of state (EoS) is here divided in two parts. The first one is devoted to the *static* EoS where the only contribution to the pressure at any given cell volume is from the electrostatic interactions among nuclei and electrons (no zero point and kinetic contributions from the vibrational motion of the atomic nuclei); the second part is devoted to the thermal equation of state where all of the contributions to the pressure are taken into account. As results for the static part are significantly dependent upon the quality of the basis set (see above the *computational details* section), at variance with those concerning the zero point and thermal pressure contributions, as it will be shown below, such separated discussion makes the issues clearer.

Always consult and cite the final, published document. See http://www.minsocam.org or GeoscienceWorld

Static Equation of State

The parameters obtained from a volume-integrated third-order Birch-Murnaghan (BM3) fitting of the static energies, calculated with the two different B1 and B2 basis sets, are reported in Table 1. With respect to the B2 basis, the B1 basis set significantly overestimates the static equilibrium cell volume and underestimates the static bulk modulus. The particularly high sensitivity of the static bulk modulus of diamond to the basis set quality was also noted by De La Pierre (2011): indeed, low quality basis sets gave lower values of the static bulk modulus than those obtained with higher quality bases (De La Pierre 2011b). The B1' basis set differs from the B1 one by having a different description of the *s* and *p* orbitals (by contrast, in B1, *s* and *p* electrons are described by *sp* shells; see above the Computational details section); this should allow a better description of the electronic distribution in the case of systems involving directional bonds, as in diamond. Such split of the *s* and *p* electrons has a small effect on the geometry, but increases the static bulk modulus by about 5 GPa (B1'/WC1LYP data in Table 1), approaching the value obtained by the B2 basis which also has splitted *s* and *p* orbital descriptions.

Static results from Zhi-Jian*et al.* (2009) are also reported in Table 1: the localized basis set they employed (B3) was a 6-21G*and the chosen functionals/Hamiltonians were the B3PW (Becke 1993; this is an hybrid Hamiltonian containing 20% of the *exact*, *non local* HF exchange), and the Hartree-Fock (RHF) one. As $K_{0,st}$ is concerned, B3PW gave results comparable to those from WC1LYP, whereas the RHF datum is largely overestimated, as it could be expected on the basis of the widely known behavior of the Hartree-Fock Hamiltonian (see for instance Prencipe and Nestola 2005). Calculations of the static bulk moduli with our B1 and B2 basis sets, and the B3PW functional (as in the work by Zhi-Jian et al. 2009), gave values of 460.3 GPa (B1/B3PW) and 476.3 GPa (B2/B3PW data in Table 1),

Always consult and cite the final, published document. See http://www.minsocam.org or GeoscienceWorld

which are to be compared with the B1/WC1LYP and B2/WC1LYP calculations (same bases, different functionals) respectively giving $K_{0,st}$=445.0 and 456.4 GPa, thus showing the significant effect of the DFT functional on such calculated elastic parameter. The increase in $K_{0,st}$, and the reduction of $V_{0,st}$ in passing from the WC1LYP to the B3PW functional is likely due to the corresponding increase of the Hartree-Fock weight in the exchange functional (16% in WC1LYP, 20% in B3PW), as it was already observed in Prencipe and Nestola (2005) in a study of the compressibility of a silicate (beryl) by means of functionals based on a B3LYP scheme, having increasingly higher HF exchange contributions.

Another paper is that from Hebbache (1999), reporting a value of 463.1 GPa for the static bulk modulus, calculated at the DFT-LDA level. A static calculation of K_0 by means of a purely DFT-GGA functional (PBE; Perdew et al. 1996), together with a plane-wave basis set and pseudopotentials, was reported by Mounet and Marzari (2005): they found a value of 432 GPa (PW/PBE data in Table 1). For comparison, in this work a calculation with the B2 basis set and the PBE Hamiltonian gave 444.02 GPa (B2/PBE data in Table 1); such difference of more than 10 GPa is very likely be attributed to differences in the basis set structure (plane-waves *vs* localized basis sets). Although, the quality of the different basis sets cannot here be judged on the basis of the agreement with the experimental data as, by definition, no zero point and thermal effects are taken into account at the static level, it is known (see next section) that such effects do decrease the bulk modulus by up to 10 GPa; in this view, *static* bulk moduli which are equal or even smaller than the experimental room temperature value (442-445GPa; Grimsditch and Ramdas 1975; Zouboulis et al. 1998) will likely be off the experimental datum by at least 10 GPa.

Smaller effects of both basis sets and Hamiltonians are observed for K'_{st} which is about 3.6.

Always consult and cite the final, published document. See http://www.minsocam.org or GeoscienceWorld

Thermal Equation of State

By adding to the static pressures (from the higher quality B2 basis set calculation) the zero point and thermal pressures estimated from the vibrational frequencies and their volume derivative (B1 and B2 calculations) of a 2x2x2 supercell of the conventional FCC diamond cell (32 k points of the reciprocal lattice, 189 normal modes of vibration), the total pressure at a given temperature could be estimated, for a set of values of the unit cell volume. For any given fixed temperature value, the P(V) data were fitted by a BM3-EoS, so that the bulk modulus K_{0T}, its pressure derivative K'_T and the equilibrium volume V_{0T} could be estimated. Results are summarized in Table 2 for the two different basis sets, at the reference temperature of 300K. The significant difference between the bulk moduli estimated by using the B1 and B2 basis sets (more than 10 GPa, as in the static calculation reported in Table 1) is due to the differences of the static contributions to the total pressure. Indeed, using the EoS parameters estimated with the B2 basis set for the static part, together with the frequencies and their volume derivatives for the vibrational part [in the latter cases, having rescaled by a factor $V_{0,st}(B2)/V_{0,st}(B1)$ the unit cell volumes at which the vibrational frequencies were calculated, being $V_{0,st}(Bx)$ the equilibrium static volume optimized by using the Bx basis set; in this way, the frequencies at any given value of the static pressure for the B1 base were assigned to cell volumes corresponding to the same static pressure for the B2 base] and fitting the resulting P(V) data, yielded a K_{0T} of 439.0GPa (V_{0T}=45.694 Å^3, K'=3.65; B1* data in Table 2), which is only about 0.7GPa higher than the bulk modulus estimated by using the frequencies calculated with the B2 basis set. This means that, even if the quality of the basis set had a significant impact on the estimated static elastic parameters, frequencies calculated with a poorer basis set could confidently be used for the evaluation of the thermal and zero point contributions to the total pressure.

Always consult and cite the final, published document. See http://www.minsocam.org or GeoscienceWorld

The reduced computational cost of the B1 basis set allowed for the calculation of vibrational frequencies also in the case of larger supercells, thus allowing a more accurate estimation of the influence of dispersion effects upon the elastic parameters. By employing the B1 basis set, the calculations of the frequencies were repeated for the 3x3x3 and 1x1x4 supercells, thus reaching a total of 148 $\underline{k}$ points having $|\underline{k}|$'s in the range $[2^{1/2}/8\ |\underline{a}^*|,\ |\underline{a}^*|]$, where $|\underline{a}^*|$ is the module of the reciprocal lattice parameter, and 885 normal modes. The distribution of the number of modes versus their frequencies (VDOS: vibrational density of states) is reported in Figure 2, whereas a drawing of the dispersion curves along the [001]* direction in the reciprocal lattice (Δ path, from the Γ toward the X point) is shown in Figure 3; the agreement with the experimental data from inelastic neutron scattering (Warren et al. 1967), which are reported in the inset of Figure 3, is quite satisfactory (in Figure 3, the frequencies for a 1x1x8 supercell calculation are also reported).

The resolution with which the reciprocal space was sampled can be measured by the value of $|\underline{k}|_{min}$: the value of modulus of the shortest sampling $\underline{k}$ vector, which is in turn connected with the size of the supercell used in the calculation of the frequencies. The impact on the bulk modulus of the increasingly larger number of sampled $\underline{k}$ points, as the resolution is increased by reducing $|\underline{k}|_{min}$ moving the correspondent $\underline{k}$ vector toward the Γ point, can clearly be seen in Figure 4, where K_0 is plotted against $|\underline{k}|_{min}$ (see also B1** data in Table 2; static parameters were from the B2 basis calculations): K_0 reaches the convergence with respect to the number of $\underline{k}$ points when $|\underline{k}|_{min}$ is smaller than about 0.77|a*| (corresponding to 59 $\underline{k}$ sampled points). No larger supercells (smaller $|\underline{k}|_{min}$) than the 3x3x3 and 1x1x4 ones are then required for an accurate evaluation of the bulk modulus, at least as phonon dispersion effects on the latter are concerned. The small variations of K_0 with $|\underline{k}|$, for $|\underline{k}|<0.77|\underline{a}^*|$, allowed us to derive an uncertainty (*precision*) of the estimated K_0 of

Always consult and cite the final, published document. See http://www.minsocam.org or GeoscienceWorld

about 0.1GPa over an average value 445.4 GPa. However, as discussed above, this datum is likely to be overestimated of almost 1 GPa with respect to the one that could be derived by using the higher quality B2 basis set for the calculation of the frequencies. In conclusion, our best estimate of K_0 for diamond at 300K was 444.6 GPa, with an uncertainty (*accuracy*: mainly due to the basis set bias) of 0.8 GPa. K' and V_0 were respectively 3.60 and 45.689 Å^3 (a_0=3.575 Å).

As usual for all the *ab initio* calculations, either at the HF/DFT or purely-DFT GGA levels, the estimated cell volumes at any pressure and temperature condition were quite overestimated with respect to the experimental ones. In other words, the curvature of the E(V) function is usually accurately estimated, at variance with the position of its minimum. The recommendation is therefore to use, in the equation of state, the experimental equilibrium cell volume at a given temperature (which is generally highly accurate), together with the calculated K_{0T} and K'_T.

Other *ab initio* estimations of the bulk modulus were available for diamond. From temperature dependent elastic constant calculations, Valdez et al. (2012) found a value of 453.54 GPa by using the purely DFT-LDA functional. Another paper by Xie et al. (1999) was devoted to the ab initio equation of state of diamond; however they did not report a numerical value of the bulk modulus at 300K, which had to be inferred from the figure they published (Figure 6 in Xie et al. 1999), where it appeared to be slightly overestimated with respect to the experimental datum. Their (LDA) results were consistent with those from Valdez et al. (2012). By employing a GGA-PBE functional (Perdew *et al*. 1996), Mounet and Marzari (2005) gave a value of 422 GPa at 300K from a volume-integrated BM4-EoS fit of their E(V) data. It should be stressed that differences in the evaluated bulk moduli from different authors were due to either the different DFT functionals employed in each case, or the basis sets, as already discussed above in the section concerning the static EoS.

Always consult and cite the final, published document. See http://www.minsocam.org or GeoscienceWorld

Experimental data from measurements of the elastic constants of diamond, at variable temperature, gave value of 442.3 GPa (Grimsditch and Ramdas 1975) and 444.8 GPa (Zouboulis et al. 1998); in the latter case, the value of the bulk modulus at 300K was obtained from a fit of $K_0(T)$ values measured in the [300, 1600K] temperature range, according to the function

$$K_0(T)= K_0(300K) + B_T(T^2-300^2) \quad (1)$$

with $K_0(300K)$ = 444.8 GPa and $B_T = -1.2\cdot10^{-5}$GPa/K^2. By performing the same fit on our $K_0(T)$ B1** data, we got $K_0(300K)$ = 443.9(4) GPa, and $B_T = -0.96(3)\cdot10^{-5}$GPa/K^2 (in parentheses are the errors from the fit). Even by considering the bias due to the basis set quality (see above), our datum fell very close and between the two experimental data available.

Isobar curves of the estimated bulk moduli as functions of temperature, in the [0, 2000K] range, are reported in Figure 5, for pressures of 0, 10, 20 and 30 GPa; as it can been seen from the Figure, all of the curves exhibited the same behavior with respect to the temperature; indeed, fitting the $K_P(T)$ data with the same quadratic function as above, gave $K_P(300K)$ = 479.5(4), 514.4(3) and 548.8(3) GPa for P = 10, 20, and 30 GPa respectively, and the same B_T values as the case of P = 0GPa [$-0.96(3)\cdot10^{-5}$ GPa/K^2].

Thermal expansion

The quasi-harmonic estimation of the thermal expansion

$$\alpha_V(T) = \frac{1}{V}\left(\frac{\partial V}{\partial T}\right)_P \quad (2)$$

Always consult and cite the final, published document. See http://www.minsocam.org or GeoscienceWorld

has been plotted in Figure 6 in the [1, 300K] temperature range. The most recent and highly accurate experimental $\alpha_V(T)$ curve from Stoupin and Shvyd'ko (2011) is also reported in the same figure. The two curves nearly overlap; in particular the difference between the calculated and experimental coefficients, at 300K ($3.19 \cdot 10^{-6}$ and $3.22 \cdot 10^{-6} K^{-1}$, respectively), is $2.7 \cdot 10^{-8} K^{-1}$, which is consistent with the accuracy of $10^{-8} K^{-1}$, estimated for the experimental measurements by Stoupin and Shvyd'ko (2011). Very good agreement exists with other literature data like those from Reeber and Wang (1996): at 300K the experimental datum for α_V is $3.05 \cdot 10^{-6} K^{-1}$ (slightly underestimated with respect to the experimental data of Stoupin and Shvyd'ko 2011); at 1000, 2000 and 3000K the experimental thermal expansion coefficients are $1.34 \cdot 10^{-5}$, $1.64 \cdot 10^{-5}$ and $1.71 \cdot 10^{-5} K^{-1}$ respectively, to be compared with the calculated data of respectively $1.25 \cdot 10^{-5}$, $1.50 \cdot 10^{-5}$ and $1.60 \cdot 10^{-5} K^{-1}$.

The very high reliability of the obtained thermal expansion, as demonstrated by the comparison of the calculated data with the experimental ones at room pressure, makes us confident about thermal expansion data at higher pressures. Figure 7 reports the calculated $\alpha_V(T)$ curves for the pressures of P=0, 10, 20 and 30 GPa, in the [0, 2000K] temperature range. As what it is frequently required is the cell volume at a given pressure and temperature [$V_P(T)$] , an empirical relation has been derived of the form:

$$\frac{V_P(T)}{V_P(300K)} = 1 + C_1 T + C_2 T^2 + C_3 T^3 + \frac{C_4}{T} + \frac{C_5}{T^2} \qquad (3)$$

where $V_P(300K)$ is the cell volume at pressure P and T=300K. This relation can confidently be used in the [300, 2500K] temperature range; the five C_i coefficients are reported in Table 3 for seven different values of the pressure in the [0, 30GPa] range. Coefficients for other values of pressure in the range can easily be derived by interpolation. As concerns other ab initio determinations of thermal

Always consult and cite the final, published document. See http://www.minsocam.org or GeoscienceWorld

expansion at high pressure and temperature, substantial agreement exists between our data and those from Xie et al. (1999), who employed an unspecified *standard* purely DFT functional, and a plane wave basis set. Ivanova and Mavrin (2013) also reported the calculation of thermal expansion of diamond in the [0, 1500K] temperature range (at the LDA-DFT level of the theory); from the plot they reported (Figure 4 in Ivanova and Mavrin 2013) it appears that $\alpha_V = 3 \cdot \alpha_L = 3.6 \cdot 10^{-6}$ K^{-1} at 300K, which is somewhat overestimated with respect to the experimental data from Reeber and Wang (1996) and Stoupin and Shvyd'ko (2011) at the same temperature ($3.22 \cdot 10^{-6}$ and $3.05 \cdot 10^{-6} K^{-1}$, respectively), but in substantial agreement with older experimental data from Slack and Bartram (1975), which they use as reference.

Again on the validity of the Quasi-Harmonic approximation

In addition to the considerations stated above in the Computational Details section about the validity of the QHA approach in deriving thermal pressures, we do stress here that the excellent agreement among the data calculated in the present work and the best experimental determinations, for just not one parameter at a given P/T condition, but for both compressibility and thermal expansion over ranges of pressure and temperature, is in itself a demonstration of the validity of QHA. Generally, failures of some algorithm in a given procedure or model are invoked when a disagreement appears between calculated and experimental data, whereas the contrary is rather unusual at least if not *lucky* random error cancellations do occur. However, such cancellations are extremely unlikely to occur at the same time for different parameters and at different P/T conditions, as in the present case.

Always consult and cite the final, published document. See http://www.minsocam.org or GeoscienceWorld

IMPLICATIONS

Diamond is a very important mineral formed in the deep mantle, and it is considered a marker of high pressure conditions at some moments during the genesis of the rocks in which it is found. In this view, the knowledge of its equation of state is fundamental (as also evidenced by the large number of publications on this subject) for any accurate quantitative estimation of the pressures involved in the rock forming processes in the Earth's mantle. More specifically, the thermoelastic parameters calculated in this work were used to calculate the pressure of formation of the diamond-olivine pair using the data by Nestola et al. 2011. In that work, the authors adopted a novel experimental approach using single-crystal X-ray diffraction to determine the internal pressure of the olivine inclusion still trapped in a diamond from Udachnaya. They claimed that the experimental approach provided a very low error in the determination of the pressure of formation, which is crucial for geobarometry purpose. While this was actually true, the only real improvement with respect to past works was relative to the determination of the internal pressure of the inclusions, whereas the other parameters used for the derivation of the pressure of formation were obtained from old literature data, which were generally affected by significant experimental uncertainties. Following the same type of calculation carried out in Nestola et al. 2011, we used the thermo-elastic parameters calculated for diamond in this work. In detail, at a fixed temperature of 1100K, the differences in the pressure of formation between the present work and that of Nestola et al. 2011, is on the third digit (3.446 GPa against 3.441 GPa, respectively) and remains of the same amount at 1600K (4.936 GPa against 4.941 GPa, respectively). This means that our calculated thermo-elastic parameters are totally consistent with the experimental ones but with the great added advantage related to the absence of any uncertainty. Our new diamond data not only could be safely used for calculation of the pressure

Always consult and cite the final, published document. See http://www.minsocam.org or GeoscienceWorld

of formation for inclusions in diamonds typical of the upper mantle, but also for those inclusions found in the so called “super deep diamonds”. Adopting our data will ensure, at the same time, reliability and absence of uncertainty resulting in a very low error in the pressure of formation derivation.

APPENDIX

Static energies and vibrational frequencies at the (static) equilibrium, and at fixed cell volumes, were performed by means of the ab initio CRYSTAL09 code (Dovesi et al. 2009), which implements the Hartree–Fock and Kohn–Sham, Self Consistent Field (SCF) method for the study of periodic systems (Pisani et al. 1988), by using a Gaussian type basis set. The present choice of the Hamiltonian and the basis set employed were discussed above in the Computational Details section. The DFT exchange and correlation contributions to the total energy were evaluated by numerical integration, over the cell volume, of the appropriate functionals; a (99, 1454)*p* grid was used, where the notation (nr, nx)p indicates a pruned grid with nr radial points and nx angular points on the Lebedev surface in the most accurate integration region (see the ANGULAR keyword in the CRYSTAL09 user’s manual, Dovesi et al. 2009). Such a grid corresponds to 2920 integration points in the unit cell at the equilibrium volume. The accuracy of the integration can be measured from the error in the integrated total electron density, which amounts to $5 \cdot 10^{-5} |e|$ for a total of 12 electrons in the cell. The thresholds controlling the accuracy of the calculation of Coulomb and exchange integrals were set to 10 (ITOL1 to ITOL4) and 22 (ITOL5; Dovesi et al. 2009). The diagonalization of the Hamiltonian matrix was performed at 16 independent $\underline{k}$ vectors in the reciprocal space (with reference to the primitive unit cell. Monkhorst net; Monkhrost and Pack 1976) by setting to 6 the shrinking factor IS (Dovesi et al. 2009).

Always consult and cite the final, published document. See http://www.minsocam.org or GeoscienceWorld

The cell parameter at the static conditions was optimized by analytical gradient methods, as implemented in CRYSTAL09 (Civalleri et al. 2001; Dovesi et al. 2009). Geometry optimization was considered converged when each component of the gradient (TOLDEG parameter in CRYSTAL09) was smaller than 0.00001 hartree/bohr and displacements (TOLDEX) with respect to the previous step were smaller than 0.00004 bohr. Static energies at each cell volume are provided as supplementary material (Table S1a and S1b, for the B1 and B2 basis sets, respectively). Vibrational frequencies and normal modes were calculated at different cell volumes, within the limit of the harmonic approximation, by diagonalizing a mass-weighted Hessian matrix, whose elements are the second derivatives of the full potential of the crystal with respect to mass-weighted atomic displacements (see Pascale et al., 2004 for details). The threshold for the convergence of the total energy, in the SCF cycles, was set to 10^{-10} hartree (TOLDEE parameter in CRYSTAL09). Results are provided as supplementary material (Tables S2a and S2b for the B1 and the B2 basis sets, respectively).

Total pressures (sum of static, zero point and thermal pressures) at different unit cell volumes and temperatures are reported as supplementary materials (Table S3).

Acknowledgements

F. Nestola and M. Bruno were supported by ERC Starting Grant 2012 (grant agreement n° 307322). M. De La Pierre acknowledges Compagnia di San Paolo for financial support (Progetti di Ricerca di Ateneo-Compagnia di San Paolo-2011-Linea 1A, progetto ORTO11RRT5).

Always consult and cite the final, published document. See http://www.minsocam.org or GeoscienceWorld

References

Aguado, F., and Baonza, V.G. (2006) Prediction of bulk modulus at high temperatures from longitudinal phonon frequencies: Application to diamond, c-BN, and 3C-SiC. Physical Review B, 73, 024111.

Becke, A. (1993) Density-functional thermochemistry. III. The role of exact exchange. Journal of Chemical Physics, 98, 5648-5652.

Civalleri, B., D'Arco Ph., Orlando, R., Saunders, V.R., and Dovesi, R. (2001) Hartree-Fock geometry optimisation of periodic systems with the CRYSTAL code. Chemical Physics Letters, 348, 131–138.

De La Pierre, M., Orlando, R., Maschio, L., Doll, K., Ugliengo, P., and Dovesi, R. (2011a) Performance of Six Functionals (LDA, PBE, PBESOL, B3LYP, PBE0, and WC1LYP) in the Simulation of Vibrational and Dielectric Properties of Crystalline Compounds. The Case of Forsterite Mg_2SiO_4. Journal of Computational Chemistry, 32, 1775–1784.

De La Pierre M. (2011b) Ab initio quantum mechanical simulation as a complementary tool for the characterization of diamond, olivines and garnets. PhD thesis, Torino, Italy.

Demichelis, R., Civalleri, B., Ferrabone, M., and Dovesi, R. (2010) On the Performance of Eleven DFT Functionals in the Description of the Vibrational Properties of Aluminosilicates. International Journal of Quantum Chemistry, 110, 406–415.

Dovesi, R., Causà, M., Orlando, R., Roetti, C., and Saunders, V.R. (1990) Ab-initio approach to molecular-crystals - a periodic Hartree-Fock study of crystalline urea. Journal of Chemical Physics, 92, 7402-7411.

Dovesi R., Orlando R., Civalleri B., Roetti C., Saunders V.R., Zicovich-Wilson C.M. (2005) CRYSTAL: a computational tool for the ab initio study of the electronic properties of crystals. Zeitschrift für Kristallographie, **220**, 571–573.

Dovesi R., Saunders V.R, Roetti C., Orlando R., Zicovich-Wilson C.M, Pascale F., Civalleri B., Doll K., Harrison N.M., Bush I.J., D'Arco Ph., Llunell M. (2009) CRYSTAL09 User's Manual, University of Torino, Torino.

Gao, G., Van Workum, K., Schall, J.D., and Harrison, J.A. (2006) Elastic constants of diamond frommolecular dynamics simulations. Journal of Physics: Condensed Matter, 18, S1737-S1750.

Grimsditch, M.H., and Ramdas, A.K. (1975) Brillouin scattering in diamond. Physical Review B, 11, 3139-3148.

Hebbache, M., (1999) First-principles calculations of the bulk modulus of diamond. Solid State Communications, 110, 559-564.

Izraeli, E.S., Harris, J.W., and Navon, O. (1999) Raman barometry of diamond formation. Earth and Planetary Science Letters, 173, 351-360.

Ivanova, T.A., and Mavrin, B.N. (2013) Ab initio Temperature Dependence of the Thermal Expansion of Diamond and the Frequency Shift of Optical Phonons. Physics of the Solid State, 55, 160-163.

Kunc, K., Loa, I., and Syassen, K. (2003) Equation of state and phonon frequency calculations of diamond at high pressures. Physical Review B, 68, 094107.

Lee C., Yang W., Parr R.G. (1988) Development of the Colle-Salvetti correlation-energy formula into a functional of the electron density. Physical Review B, **37**, 785–789.

Maezono, R., Ma, A., Towler, M.D., and Needs, R.J. (2007) Equation of State and Raman Frequency of Diamond from Quantum Monte Carlo Simulations. Physical Review Letters, 98, 025701.

Always consult and cite the final, published document. See http://www.minsocam.org or GeoscienceWorld

McSkimin, H.J., and Andreatch, P. (1972) Elastic Moduli of Diamond as a Function of Pressure and Temperature. Journal of Applied Physics, 43, 2944-2948.

Monkhrost, H.J., and Pack, J.D. (1976) Special points for Brillouin-zone integration. Physical Review B, 8, 5188–5192.

Mounet, N., and Marzari, N. (2005) First-principles determination of the structural, vibrational and thermodynamic properties of diamond, graphite, and derivatives. Physical Review B, 71, 205214.

Nestola, F., Nimis, P., Ziberna, L., Longo, M., Marzoli, A., Harris, J.W., Manghnani, M.H., and Fedortchouk, Y. (2011) First crystal-structure determination of olivine in diamond: Composition and implications for provenance in the Earth's mantle. Earth and Planetary Science Letters, 305, 249-255.

Pascale, F., Zicovich-Wilson, C.M., Lopez Gejo, F., Civalleri, B., Orlando, R., and Dovesi, R. (2004) The calculation of the vibrational frequencies of crystalline compounds and its implementation in the CRYSTAL code. Journal of Computational Chemistry, 25, 888–897.

Peintinger, M.F., Vilela Oliveira, D., and Bredow, T. (2013) Consistent Gaussian Basis Sets of Triple-Zeta Valence with Polarization Quality for Solid-State Calculations, Journal of Computational Chemistry, 34, 451-459.

Perdew, J.P., Burke, K., and Ernzerhof, M. (1996) Generalized gradient approximation made simple. Physical Review Letters, 77, 3865–3868.

Pisani, C., Dovesi, R., and Roetti, C. (1988) Hartree-Fock ab initio treatment of crystalline systems. Lecture notes in chemistry, 48. Springer, Berlin, Heidelberg, New York

Prencipe M., Nestola F. (2005) Quantum-mechanical modeling of minerals at high pressures. The role of the Hamiltonian in a case study: the beryl ($Al_4Be_6Si_{12}O_{36}$). Physics and Chemistry of Minerals, 32, 471-479.

Prencipe, M., Scanavino, I., Nestola, F., Merlini, M., Civalleri, B., Bruno, M., and Dovesi, R. (2011) High-pressure thermo-elastic properties of beryl (Al4Be6Si12O36) from ab initio calculations, and observations about the source of thermal expansion. Physics and Chemistry of Minerals, 38, 223–239.

Prencipe, M. (2012a) Simulation of vibrational spectra of crystals by ab initio calculations: an invaluable aid in the assignment and interpretation of the Raman signals. Journal of Raman Spectroscopy, 43, 1567-1569.

Prencipe, M., Mantovani, L., Tribaudino, L., Bersani, D., and Lottici, P.L. (2012b) The Raman spectrum of diopside: a comparison between ab initio calculated and experimentally measured frequencies. European Journal of Mineralogy, 24, 457-464.

Reeber, R.R., and Wang, K. (1996) Thermal Expansion, Molar Volume and Specific Heat of Diamond from 0 to 3000K. Journal of Electronic Materials, 25, 63-67.

Scanavino, I., Belousov, R., and Prencipe, M. (2012) Ab initio quantum-mechanical study of the effects of the inclusion of iron on thermoelastic and thermodynamic properties of periclase (MgO). Physics and Chemistry of Minerals, 39, 649–663.

Scanavino, I., and Prencipe, M. (2013) Ab-initio determination of high pressure and high temperature thermoelastic and thermodynamic properties of low-spin ($Mg_{1-X}Fe_X$)O ferropericlase with x in the range [0.06, 0.59]. American Mineralogist, 98, 1270-1278.

Shirey, S.B., Cartigny, P., Frost, D.J., Keshav, S., Nestola, F., Nimis, P., Pearson, D.G., Sobolev, N.V., and Walter, M.J. (2013) Diamonds and the Geology of Mantle Carbon. Reviews in Mineralogy & Geochemistry, 75, 355-421.

Always consult and cite the final, published document. See http://www.minsocam.org or GeoscienceWorld

Slack, G.A., and Bartram, S.F. (1975) Thermal expansion of some diamond like crystals. Journal of Applied Physics, 46, 89-98.

Stachel, T., Harris, J.W., 2008. The origin of cratonic diamonds — constraints from mineral inclusions. Ore Geology Reviews, 34, 5–32.

Stoupin, S., and Shvyd'ko, Y.V. (2011) Ultraprecise studies of the thermal expansion coefficient of diamond using backscattering x-ray diffraction. Physical Review B, 83, 104102.

Ungureanu, C.G., Cossio, R., and Prencipe, M. (2010) Thermodynamic properties of CaCO3 aragonite at high pressure: An ab-initio quantum-mechanical calculation. European Journal of Mineralogy, 22, 693–701.

Ungureanu, C.G., Cossio, R., and Prencipe, M. (2012) An Ab-initio assessment of thermo-elastic properties of CaCO3 polymorphs: Calcite case. Calphad, 37, 25–33.

Valdez, M.N., Umemoto, K., and Wentzcovitch, R.M. (2012) Elasticity of diamond at high pressures and temperatures. Applied Physics Letters, 101, 171902.

Vogelgesang, R., Ramdas, A.K., Rodriguez, S., Grimsditch, M., and Anthony, T.R. (1996) Brillouin and Raman scattering in natural and isotopically controlled diamond. Physical Review B, 54, 3989-3999.

Warren, J.L., Yarnell, J.L., Dolling, G., and Cowley, R.A. (1967) Lattice Dynamics of Diamond. Physical Review, 158, 805-808.

Wu, Z., and Cohen, R. (2006) More accurate generalized gradient approximation for solids. Physical Review B, 73, 2–7.

Xie, J., Chen, S.P., and Tse, J.S. (1999) High-pressure thermal expansion, bulk modulus, and phonon structure of diamond. Physical Review B, 60, 9444-9449.

Zhi-Jian F., Guang-Fu J., Xiang-Rong C, and Qing-QuanG. (2009) First-Principle Calculations for Elastic and Thermodynamic Properties of Diamond. Communication in Theoretical Physics, **51**, 1129–1134.

Zicovich-Wilson, C.M., Pascale, F., Roetti, C., Saunders, V.R., Orlando, R., and Dovesi, R. (2004) Calculation of the vibration frequencies of alpha-quartz: the effect of Hamiltonian and basis set. Journal of Computational Chemistry, 25, 1873–81.

Zouboulis, E.S., Grimsditch, M., Ramdas, A.K., and Rodriguez, S. (1998) Temperature dependence of the elastic moduli of diamond: A Brillouin-scattering study. Physical Review B, 57, 2889-2896.

Zucchini, A., Prencipe, M., Comodi, P., and Frondini, F. (2012) Ab initio study of cation disorder in dolomite. CALPHAD: Computer Coupling of Phase Diagrams and Thermochemistry, 38, 177–184.

Always consult and cite the final, published document. See http://www.minsocam.org or GeoscienceWorld

Captions to the Tables:

Table 1: Static cell volume ($V_{0,st}$; in Å^3) and cell parameter ($a_{0,st}$; in Å) at the static equilibrium (P_{st}=0); static bulk moduls ($K_{0,st}$; in GPa) and its pressure derivative (K'_{st}), obtained with different basis sets/Hamiltonians (see text for explanations concerning both the basis sets and the Hamiltonians).

Table 2: Equilibrium cell volume (V_{0T}; in Å^3) and cell parameter (a_{0T}; in Å); bulk moduls (K_{0T}; in GPa) and its pressure derivative (K'_T), at the temperature of 300K, calculated with different basis sets (WC1LYP functional).

Table 3: Coefficients of the equation (3) for the interpolation of the ratio $V_P(T)/V_P(300K)$ at several pressures, in the [300, 2500K] temperature range. See text for explanations. C_1 is in K^{-1}, C_2 in K^{-2}, C_3 in K^{-3}, C_4 in K and C_5 in K^2.

Captions to the Figures:

Figure 1: Scan of the total energy (in hartree) along the normal mode coordinate (Q) corresponding to a vibrational mode at 283 cm^{-1}; Q has been given in unit Q_{max}: the maximum displacement, evaluated at the classical level, corresponding to the energy of the quantum ground state.

Figure 2: Vibrational density of state of diamond (VDOS). See text for explanation.

Figure 3: Phonon dispersion in diamond along the [001]* path in the reciprocal space (Δ path), from the Γ point (Brillouin zone center) to the X point (zone border). The inset represents the experimental data along the same path, from the work of Warren et al., 1967. Reprinted excerpt with permission from Warren, J.L., Yarnell, J.L., Dolling, G., and Cowley, R.A., Physical Review, 158, 805, 1967. Copyright (1967) by the American Physical Society.

Figure 4: Bulk modulus at 300K (K_0 in GPa) as a function of the size of the supercell employed for the calculation, the latter being measured by the module of the corresponding smallest $\underline{k}$ vector (in unit of $|\underline{a}^*|$). Note that $|\underline{k}|$=1 $|\underline{a}|^*$ corresponds to a vector of the reciprocal lattice, which is therefore equivalent to the Γ point.

Figure 5: Bulk modulus (K_p) as a function of temperature, at four different pressures (isobar curves).

Figure 6: Thermal expansion coefficient (α_V; referred to the volume of the unit cell) as a function of temperature (low temperature data). The experimental data (dashed curve) are from the fit as it is reported in Stoupin and Shvyd'ko (2011).

Figure 7: Thermal expansion coefficient (α; referred to the unit cell volume) as a function of temperature, at four different pressures (isobar curves).

Always consult and cite the final, published document. See http://www.minsocam.org or GeoscienceWorld

Tables

Table 1

Basis set/Hamiltonian	$V_{0,st}$	$a_{0,st}$	$K_{0,st}$	K'_{st}
B1/WC1LYP	45.872	3.5797	445.0	3.62
B1'/WC1LYP	45.878	3.5799	450.3	3.58
B2/WC1LYP	45.187	3.5618	456.4	3.62
B1/B3PW	45.478	3.5694	460.3	3.62
B2/B3PW	44.793	3.5514	476.3	3.61
B2/PBE	45.477	3.5694	444.0	3.66
B3/B3PW[a]	45.526	3.5707	442.8	3.43
B3/RHF[a]	45.358	3.5663	508.7	3.58
PW/PBE[b]	45.432	3.5682	432	-

[a]Zhi-Jian*et al*. (2009)
[b]Mounet and Marzari (2005)

Table 2

	V_{0T}	a_{0T}	K_{0T}	K'_{T}
B1	46.399	3.5934	427.7	3.65
B2	45.717	3.5757	438.3	3.66
B1*	45.694	3.5751	439.0	3.65
B1**	45.689	3.5750	445.4	3.60

Table 3

P	$c_1 (x10^{6})$	$c_2 (x10^{9})$	$c_3 (x10^{13})$	c_4	c_5
0	2.78	5.62	-8.47	-1.48	330.61
5	2.57	5.47	-8.26	-1.41	316.17
10	2.37	5.33	-8.07	-1.34	302.75
15	2.19	5.20	-7.90	-1.28	290.18
20	2.03	5.07	-7.72	-1.22	278.52
25	1.88	4.95	-7.55	-1.17	267.50
30	1.74	4.83	-7.39	-1.12	257.44

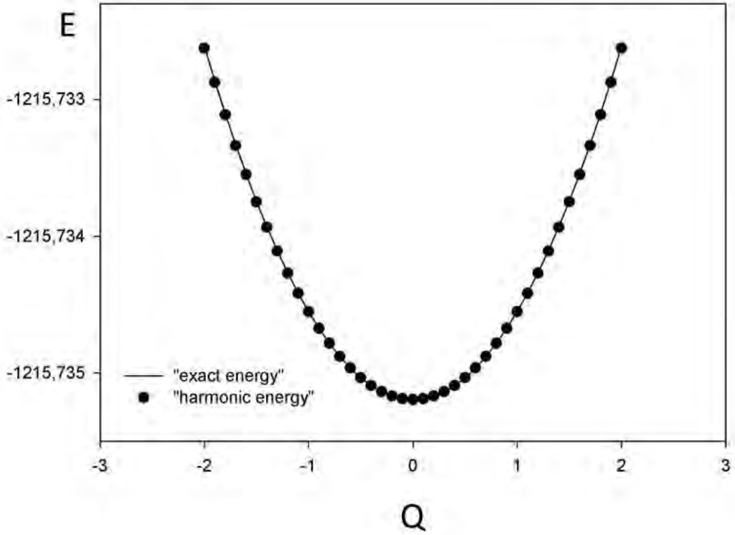
E
-1215,733
-1215,734
-1215,735
"exact energy"
"harmonic energy"
-3
-2
-1
0
1
2
3
Q

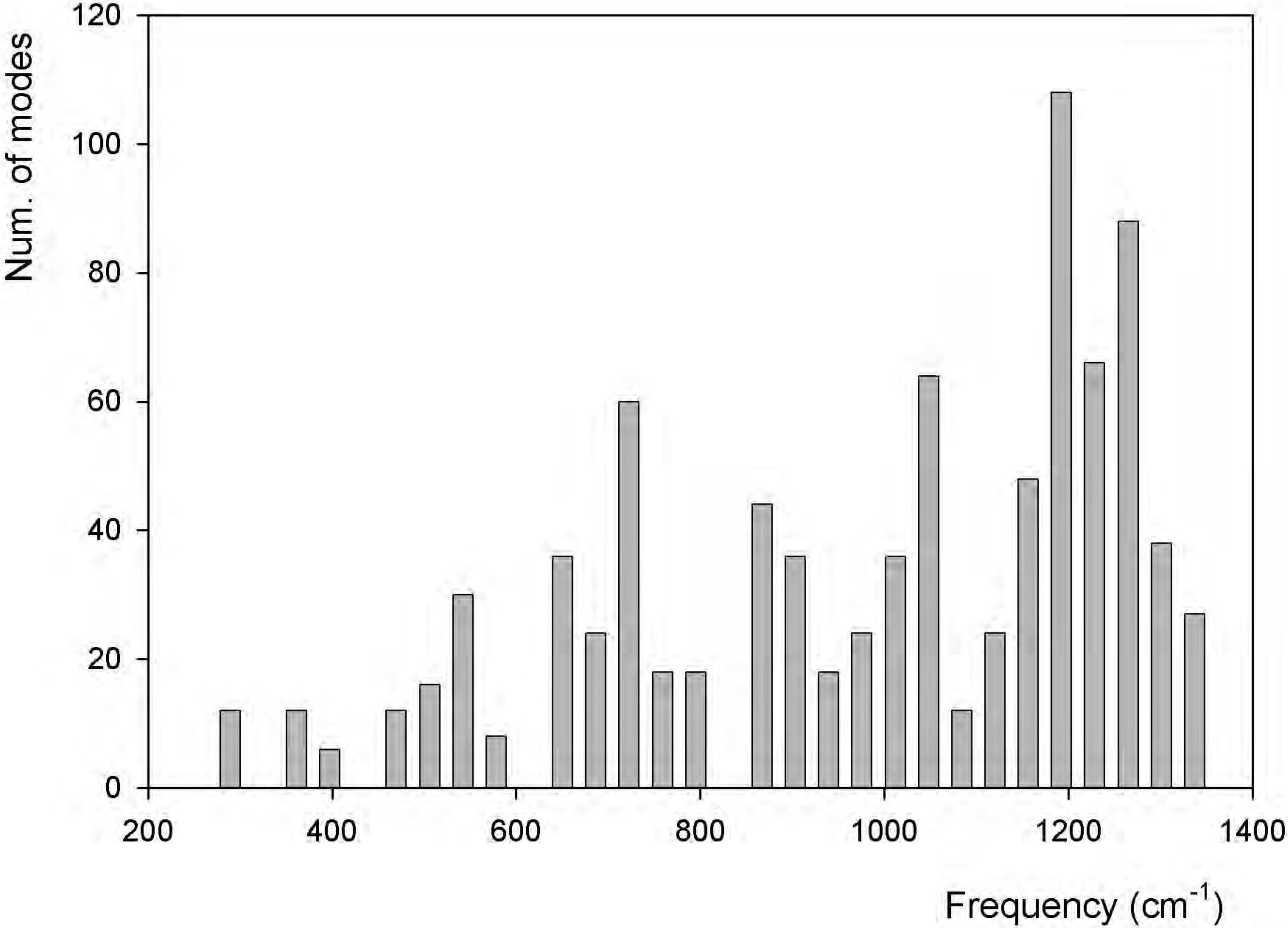

Num. of modes
0
20
40
60
80
100
120
200
400
600
800
1000
1200
1400
Frequency (cm-1)

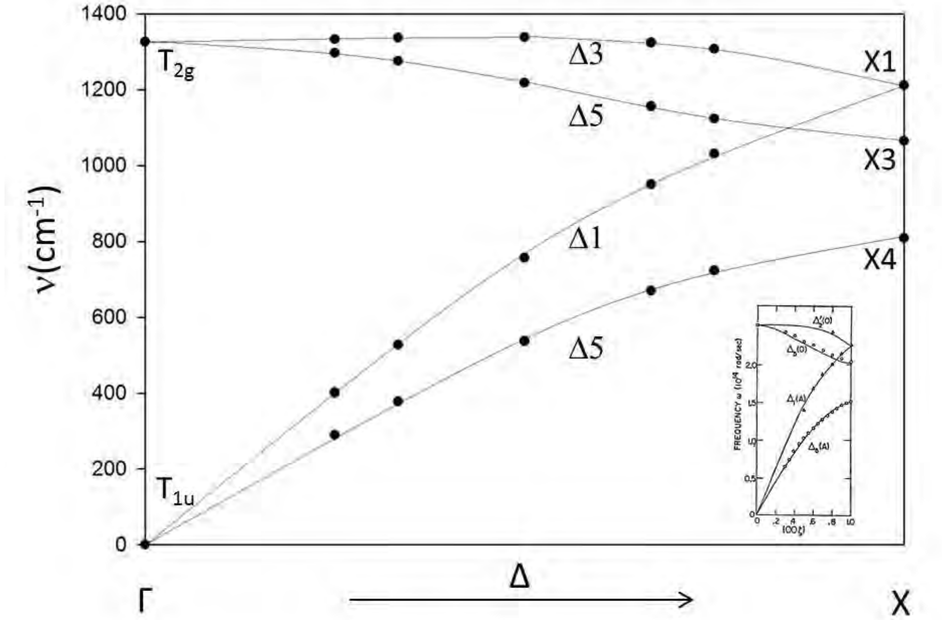

1400
1200
1000
800
600
400
200
0
ν(cm-1)
T2g
T1u
Δ3
Δ5
Δ1
Δ5
X1
X3
X4
Γ
Δ
X

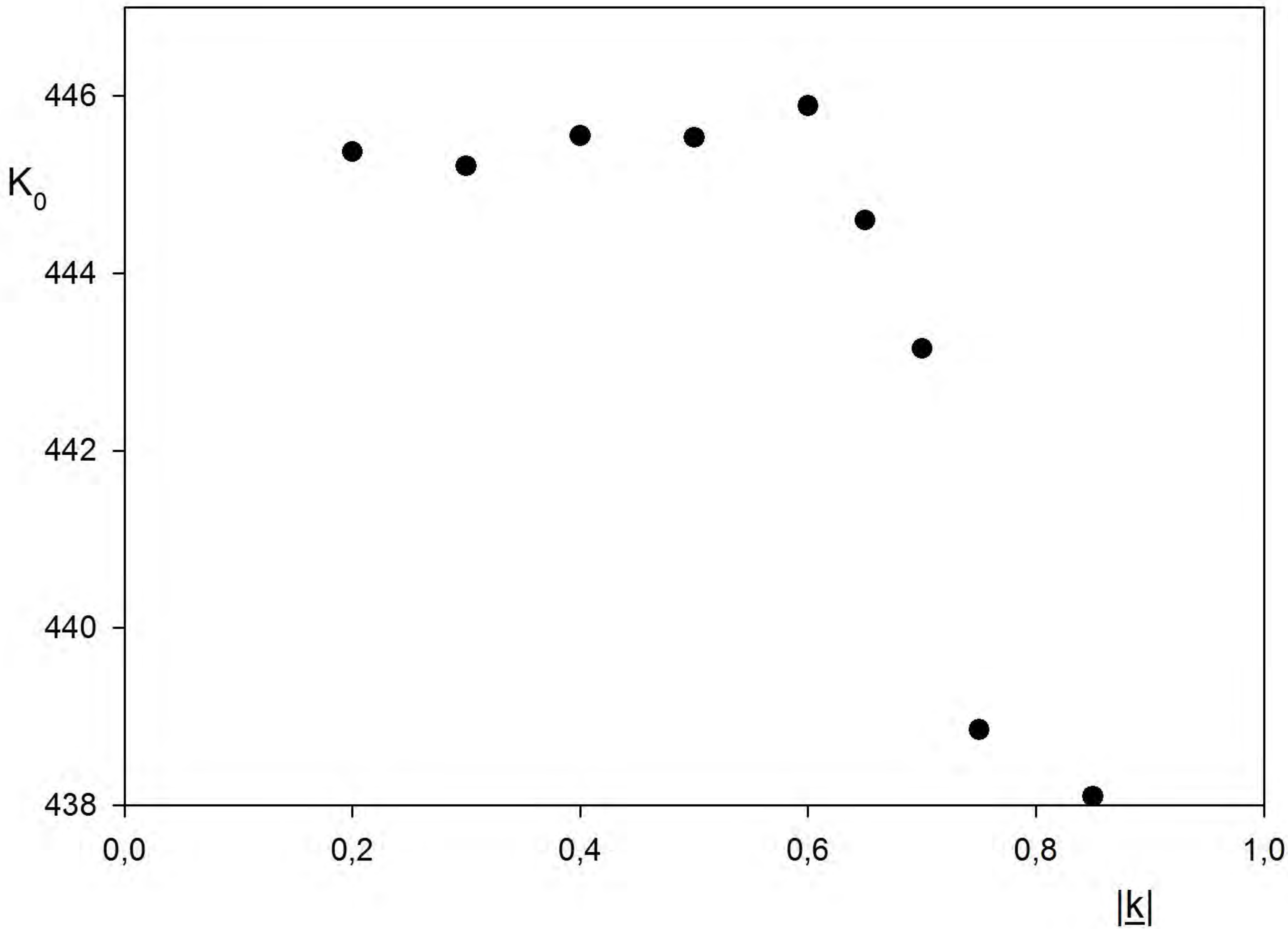

446
444
442
440
438
K_0
0,0
0,2
0,4
0,6
0,8
1,0
$|\underline{k}|$

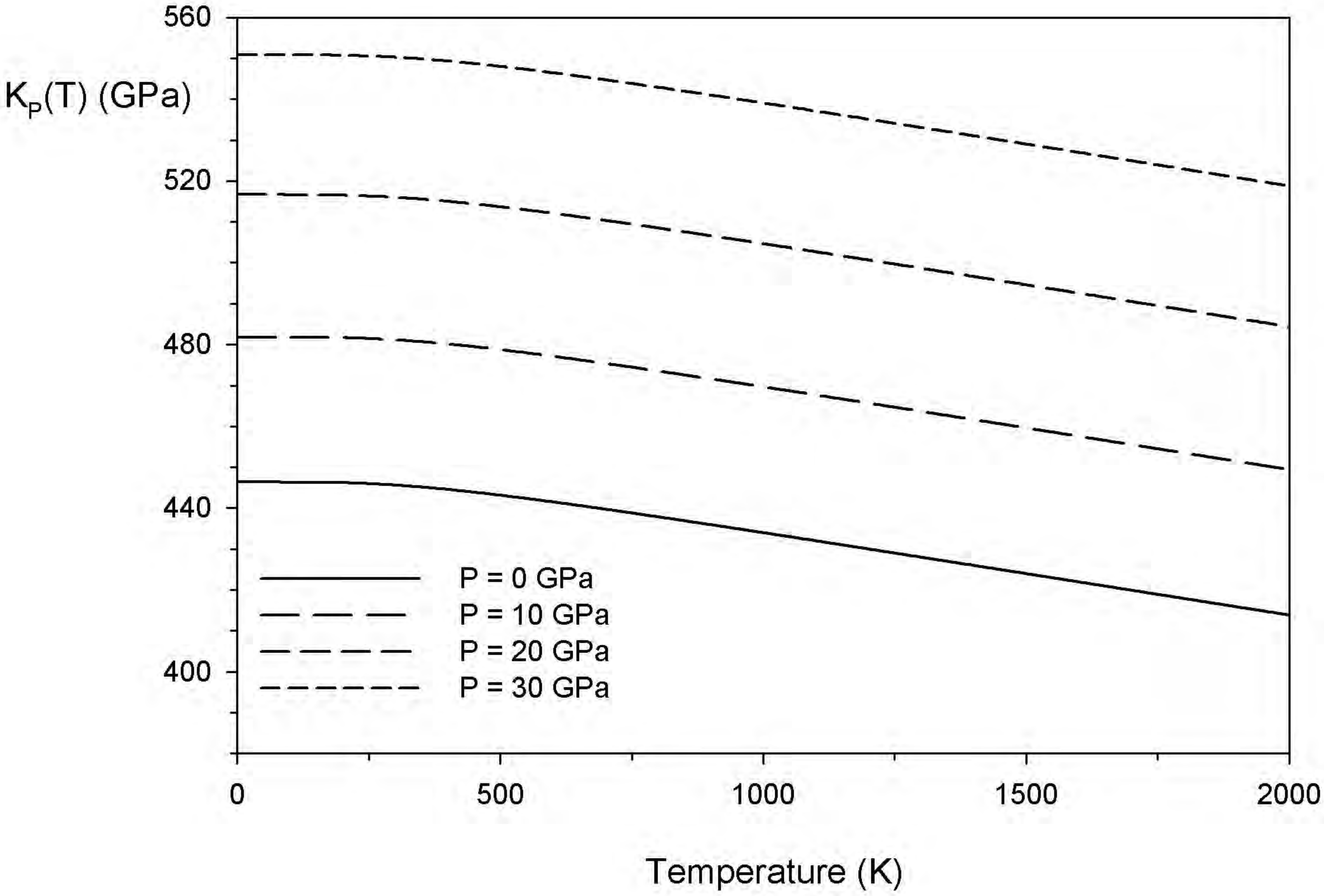
560
520
480
440
400
$K_P(T)$ (GPa)
P = 0 GPa
P = 10 GPa
P = 20 GPa
P = 30 GPa
0
500
1000
1500
2000
Temperature (K)

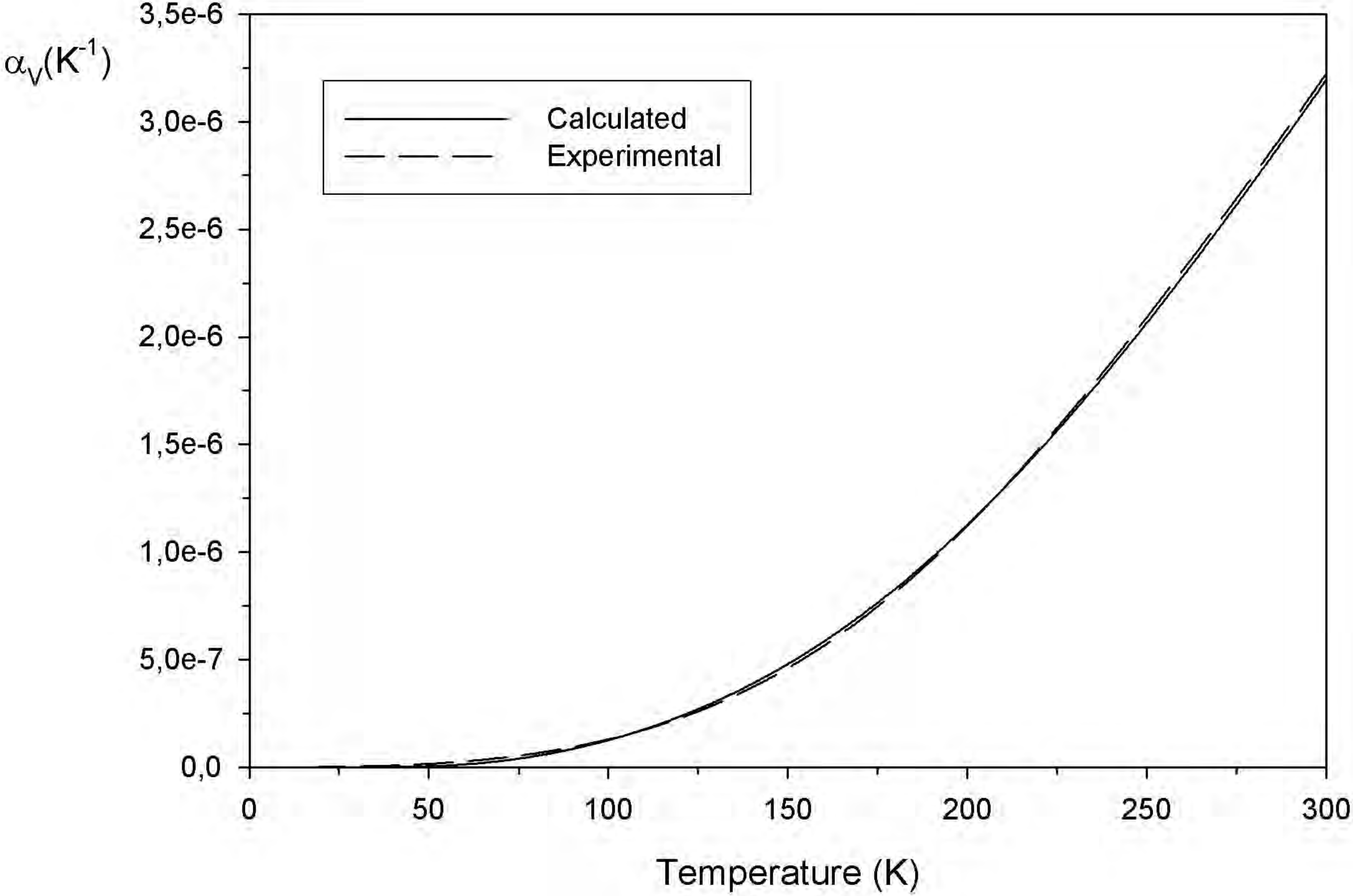

$\alpha_V(K^{-1})$
3,5e-6
3,0e-6
2,5e-6
2,0e-6
1,5e-6
1,0e-6
5,0e-7
0,0
0
50
100
150
200
250
300
Temperature (K)
Calculated
Experimental

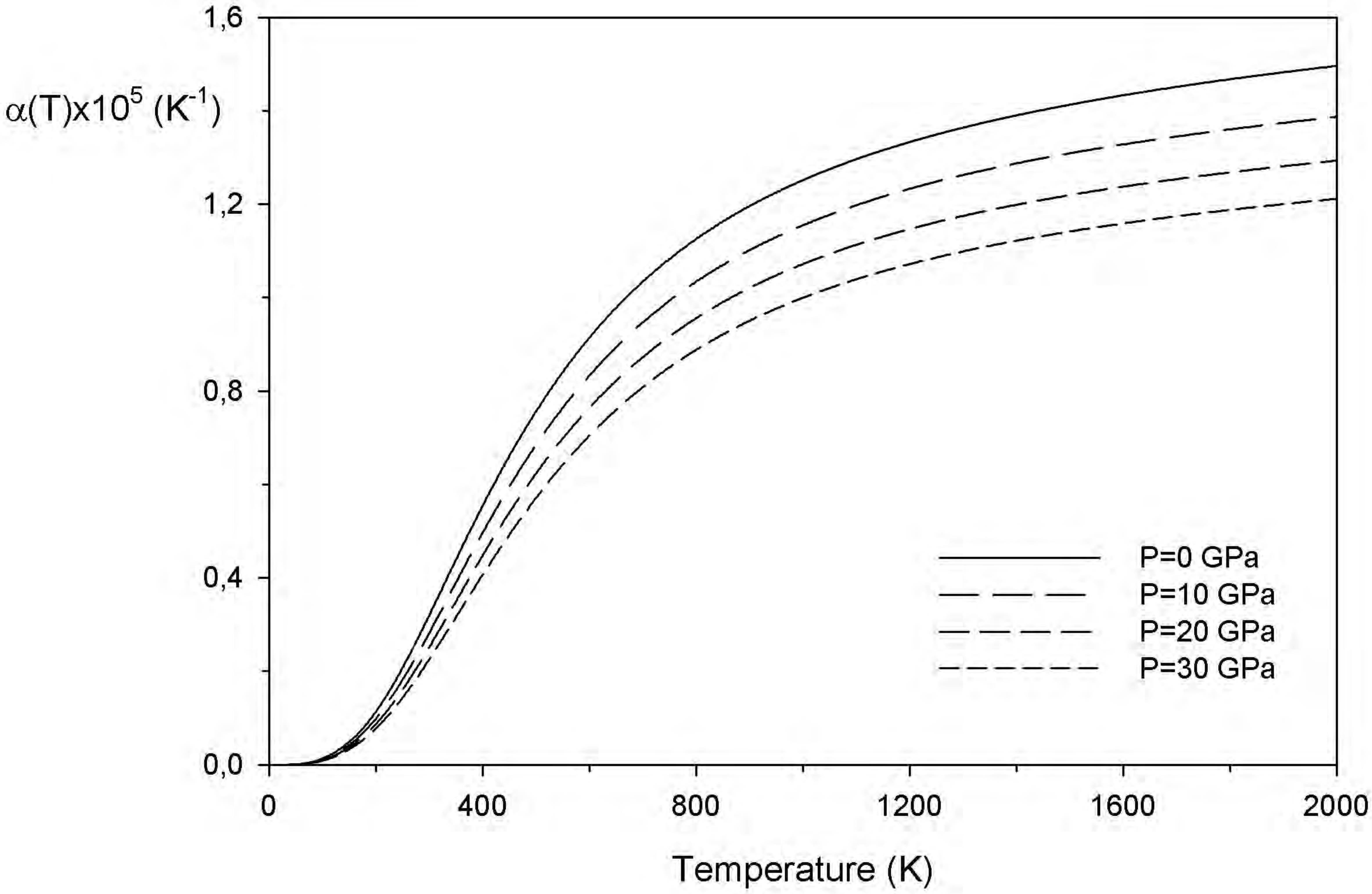

α(T)x10^5 (K^-1)
1,6
1,2
0,8
0,4
0,0
0
400
800
1200
1600
2000
Temperature (K)
P=0 GPa
P=10 GPa
P=20 GPa
P=30 GPa